Experimental and Theoretical Charge Density Study of the Chemical Bonding in Chlorokojic Acid Crystal Structure

ARTICLE *in* THE JOURNAL OF PHYSICAL CHEMISTRY A · SEPTEMBER 2012

Impact Factor: 2.69 · DOI: 10.1021/jp3058614 · Source: PubMed

2 AUTHORS, INCLUDING:

Anna Krawczuk
Jagiellonian University
17 PUBLICATIONS **68** CITATIONS

SEE PROFILE

THE JOURNAL OF PHYSICAL CHEMISTRY A

Article

pubs.acs.org/JPCA

Experimental and Theoretical Charge Density Study of the Chemical Bonding in Chlorokojic Acid Crystal Structure

Anna Krawczuk* and Katarzyna Stadnicka

Faculty of Chemistry, Jagiellonian University, Ingardena 3, 30-060 Krakow, Poland

Supporting Information

ABSTRACT: The experimental charge density in the chlorokojic acid crystal structure was investigated on the basis of high-resolution X-ray diffraction data collected at 80(2) K. The nature of chemical bonding and halogen interactions has been studied by means of deformation densities and by topological analysis using the Bader's quantum theory of atoms in molecules (QTAIM). A comparison between the experimental and theoretical results, from calculations concerning gas phase and periodic DFT/B3LYP, was performed. For the intermolecular hydrogen bonds of O–H···O, C–H···O, and C–H···Cl types, full characteristics of bond critical points (BCP's) were provided indicating closed-shell interactions. The topological analysis of charge density distribution revealed the presence of intermolecular C–Cl···O halogen bridge and halogen–halogen interactions of C–Cl···Cl–C type forming supramolecular Cl_3 synthons, crucial for three-dimensional structure formation of chlorokojic acid. The pronounced anisotropy of electrostatic potential at the Cl atom clarifies both electrophilic and nucleophilic properties of the substituent.

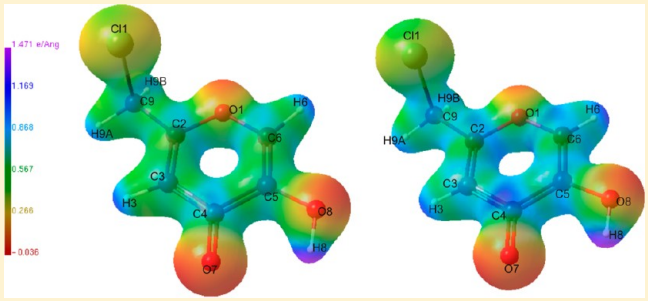

1. INTRODUCTION

In the last years, studies on chemical bonding using the Bader's[1] quantum theory of atoms in molecules (QTAIM) have been an active topic of research.[2−6] The QTAIM methodology is a powerful tool to analyze and interpret the electron densities obtained from high-resolution X-ray diffraction or theoretically calculated from quantum wave functions. Electron properties at the bond critical point (BCP), which lies along the bond path with the gradient of electron density equal to zero, are extensively used for the characterization of interatomic interactions from electron density distribution. The trace of Hessian 3 × 3 symmetric matrix, Laplacian $\nabla^2\rho(\mathbf{r})$, together with principal curvatures (Hessian matrix eigenvalues) computed at the BCP are often used to characterize the chemical interactions within a molecule or crystal. The negative value of Laplacian indicates the local concentration of the density resulting in shared interaction, whereas the positive value of Laplacian represents the local depletion of electron density, which leads to closed-shell interactions.[7] This relationship may also be introduced by the correlation of electronic parameters at BCP with the local electronic kinetic $G(\mathbf{r}_c)$ and local potential $V(\mathbf{r}_c)$ energies and hence to the total local energy density $E(\mathbf{r}_c)$.[8,9] The full description of this approach will be introduced later in the article.

Chlorokojic acid itself is known to be biologically active; like many other derivatives of kojic acid, it indicates antimicrobial and antifungal properties.[10,11] As a chemical compound, chlorokojic acid is a good ligand for the nucleophilic substitution reactions depending on the reagent type.[12−14] If secondary amines as the nucleophiles for the substitution are used, the carbon atom 6 in pyran ring is attacked. When I^- or SCN^- are used, the chlorine atom is simply replaced by the anions. Chlorokojic acid as a bidentate chelating ligand forms stable complexes with metal ions. It was shown that such complexes have an inhibitory effect on the growth of *Aeromonas aerogenes*, *Salmonella typhosa*, *Penicilium digitalum*, *Russula nigricans*, and *Accharomyces cerevisiae*.[15] Moreover, such complexes were tested as new drugs in the therapy of diabetes and anemia.[16,17]

The crystal structure of chlorokojic acid at low-temperature (100 K) and vibrational spectra were previously reported.[18] It was shown that chlorine atoms may form a pseudohexagonal arrangement with folded layers at 1/4, *y*, *z* and 3/4, *y*, *z*. It was also pointed out that, in the crystal structure, a few hydrogen bonds are present: three intermolecular ones O8–H8···O7 ($-x + 1, -y + 1, z + 1/2$), C3–H3···O7 ($-x + 1, -y + 1, z - 1/2$), and C6–H6···Cl1 ($x, y, z + 1$), and one intramolecular O8–H8···O7. Additionally, a particularly short contact between O1 atom from the pyran ring and the chlorine atom at $-x + 1/2, y + 1/2, z - 1/2$ was observed (3.079 Å). To provide the insight into the charge density distribution within the chlorokojic acid molecule and the intermolecular interactions, especially those of possible halogen interactions of C–Cl···Cl

Received: June 14, 2012
Revised: September 3, 2012

   dx.doi.org/10.1021/jp3058614 | *J. Phys. Chem. A* XXXX, XXX, XXX–XXX

and C−Cl···O types, we herein present combined experimental and theoretical studies of the chlorokojic acid.

2. EXPERIMENTAL SECTION

The synthesis of chlorokojic acid was performed using procedures described earlier.[19] Colorless crystals were obtained by slow evaporation from aqueous solution of chlorokojic acid. The crystal was cooled from ambient temperature to 80 K using Oxford 700 Series Cryostream Cooler. The measurement was performed on Nonius KappaCCD diffractometer running under Nonius *COLLECT* software.[20] A total of two runs were recorded using ω scans at $\chi = 55°$. In the main run (θ_{max} = 53.87°, scan width = 0.300°/frame), a total number of 1483 images were collected with exposure time of 0.75 min per frame, whereas in the additional run (θ_{max} = 27.48°, scan width = 1.200°/frame, total number of 138 images), the exposure time 0.40 min/frame was used to measure high-intensity low-angle data more accurately. Cell parameters and data processing were performed using HKL DENZO and Scalepack.[21] Absorption corrections were introduced using multiscan procedure.[21] A total of 14 610 reflections were sorted and merged using SORTAV,[22] giving 6401 independent data in the *mm*2 crystal class.

2.1. Spherical Refinement. A spherical atom refinement according to SHELXL-97,[23] with full-matrix least-squares on F^2 using all data, was performed. Space group $Pna2_1$ was assigned from the systematic absences observed in the diffraction pattern and the results of $|E|$ distribution and $N(z)$ test clearly indicated the noncentrosymmetric space group. All non-H atoms were allowed anisotropic thermal motion. Hydrogen atoms of the methylene and aromatic C−H groups were found on the difference Fourier map and included in the refinement in geometrically calculated positions (methylene C−H = 0.99 Å, aromatic C−H = 0.95 Å) with $U_{iso}(H) = 1.2U_{eq}$ (parent C). The hydrogen atom of hydroxyl group was found on the difference Fourier map and refined in a riding model with $U_{iso}(H) = 1.5U_{eq}$ (parent O) without constrains. For structural drawings, Ortep-3 for Windows[24] was used. All calculations were carried out using WinGX package suite.[25] Selected crystal data and experimental details are shown in Table 1.

2.2. Multipole Refinement. The multipole formalism of Hansen and Coppens[26] implemented in the XD2006 program package[27] was used. The aspherical atom electron density is given by

$$\rho(\mathbf{r}) = \rho_c(\mathbf{r}) + P_v\kappa^3\rho_v(\mathbf{r}) + \sum_{l=0}^{lmax} \kappa^3 R_l(\kappa'\mathbf{r}) \sum_{m=0}^{l} P_{lm\pm} y_{lm\pm}(\theta, \phi)$$

where $\rho_c(\mathbf{r})$ and $\rho_v(\mathbf{r})$ are core and spherical valence densities, respectively, $y_{lm\pm}$ represents spherical harmonic angular functions, R_l is the radial function, κ and κ' are the expansion/contraction parameters, and P_v and $P_{lm\pm}$ represent the population parameters. The function minimized in the least-squares procedure was $\sum w(|F_o| - k|F_c|)^2$, only those reflections with $|F_o| > 2\sigma(F_o)$ were included in the refinement. Initially, the scale factor was refined against all data. The high-order refinement ($\sin\theta/\lambda \geq 0.7$ Å^{-1}) for non-H atoms was performed in order to obtain optimal positional and thermal parameters. The low-order refinement ($\sin\theta/\lambda \leq 0.7$ Å^{-1}) was carried out to receive accurate thermal parameters for hydrogen atoms. The hydrogen positional parameters were fixed at the neutron determined distances of 1.09 Å for the methylene

Table 1. Crystal Data and Experimental Details for Chlorokojic Acid

	chlorokojic acid
Crystal Data	
chemical formula	$C_6H_5ClO_3$
MW	160.55
crystal system, space group	orthorhombic, $Pna2_1$
a, b, c (Å)	20.4155(4), 4.2843(1), 7.2499(1)
temperature (K)	80(2)
V (Å^3)	634.12(2)
Z	4
D_x (gcm^{-3})	1.682
$F(000)$	328
radiation type, λ (Å)	MoKα, 0.71073
μ (mm^{-1})	0.535
crystal form, color	plate, colorless
crystal size (mm)	0.62 × 0.25 × 0.07
Data Collection	
diffractometer	Nonius Kappa CCD
data collection method	ω scans at χ=55°
absorption correction	multiscan[21]
no. of reflections measured/ independent	14610/6401
R_{int}	0.021
θ range (deg)	3.45−53.35
Spherical Atom Refinement	
no. of data in refinement/with $F^2 > 2\sigma(F^2)$	6401/5397
no. of parameters	94
flack parameter[55]	0.0(2)
$R[F^2 > 2\sigma(F^2)]$ (all data)/$wR(F^2)$ (all data) (S)	0.035 (0.0469)/0.079 (0.085) /1.026
ρ_{min}/ρ_{max}/rms (e·Å^{-3})	−0.398/0.492/0.074
Multipolar Refinement	
no. of data in refinement/$F > 2\sigma(F)$	6401/5633
no. of refined parameters	294
$R[F > 2\sigma(F)]$ (all data)/$Rw(F)$	0.022 (0.045)/0.022
R ($\sin\theta/\lambda \leq 0.7$ Å^{-1})	0.014
goodness-of-fit	1.155
N_{ref}/N_v	13.63
max shift/esd in last cycle	<10^{-4}
ρ_{min}/ρ_{max}/rms (e·Å^{-3}) ($\sin\theta/\lambda \leq 0.7$ Å^{-1})	−0.240/0.265/0.057 (−0.166/0.126/0.035)

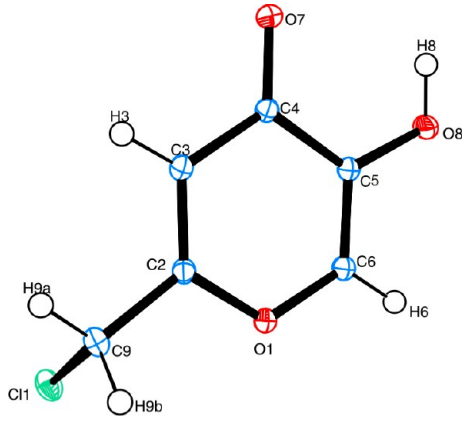

Figure 1. Ortep-3 view of the chlorokojic acid molecule with labeling scheme. Displacement ellipsoids are drawn at the 50% probability level.

dx.doi.org/10.1021/jp3058614 | J. Phys. Chem. A XXXX, XXX, XXX−XXX

Table 2. Comparison of Selected Bond Lengths (Å) and Angles (deg) from Experimental and Theoretical Studies of Chlorokojic Acid

	exptl[a]	exptl[18]	B3LYP[18]/6-31+G**	B1LYP[40]/6-311++G(d,p)	BLYP[40]/6-311++G(p,d)
O1−C2	1.347(1)	1.353(2)	1.350	1.346	1.366
O1−C6	1.360(1)	1.359(2)	1.366	1.363	1.379
O7−C4	1.248(1)	1.243(2)	1.241	1.232	1.251
O8−C5	1.348(1)	1.350(2)	1.347	1.345	1.356
C2−C3	1.355(1)	1.348(2)	1.360	1.354	1.369
C2−C9	1.489(1)	1.486(2)	1.492	1.490	1.494
C3−C4	1.446(1)	1.448(2)	1.447	1.447	1.451
C4−C5	1.456(1)	1.456(2)	1.469	1.468	1.477
C5−C6	1.356(1)	1.352(2)	1.354	1.348	1.326
C9−Cl1[b]	1.800(1)	1.804(1)	1.823	1.822	1.855
Cl1−C9−C2	109.95(6)	109.8(1)	112.0	111.7	111.83

[a]This work. [b]Uncorrected distance 1.7993, lower bound 1.7995, upper bound 1.8317, riding motion 1.8019, and noncorrelated motion 1.8156 Å; as calculated by Parst[41] following Busing and Levy.[42]

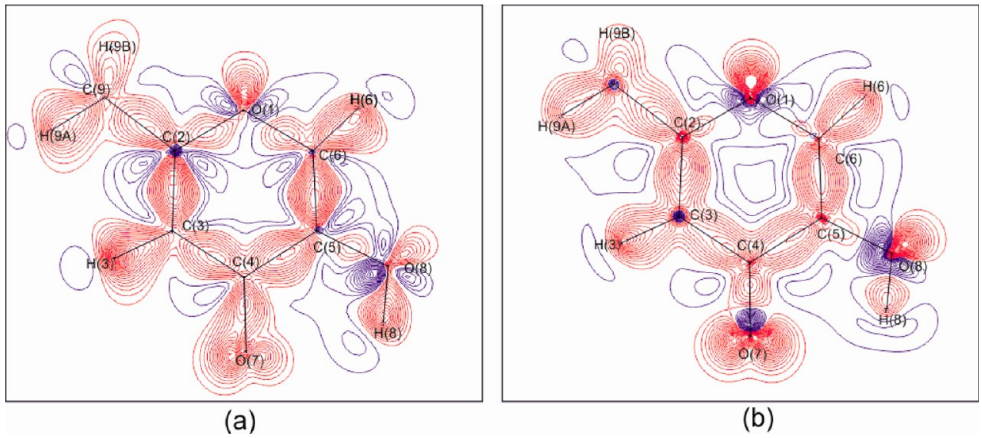

Figure 2. Static deformation charge density distribution of chlorokojic acid in the plane of pyran ring from experimental (a) and periodic calculations (b) studies. The positive (solid red lines) and negative (solid blue lines) contours are drawn at intervals 0.05 e·Å^{-3}.

group, 1.08 Å for aromatic C−H groups, and 0.95 Å for hydroxyl O−H group.[28] In the absence of neutron diffraction data, the H-atom anisotropic displacement parameters (ADPs) were estimated by using the SHADE2 web server,[29,30] and the obtained values were subsequently kept fixed during the refinement. The multipole expansion was truncated at the hexadecapole level for Cl atom, octapole level for the C and O atoms. In the case of H atoms, the multipole expansion was kept up to the quadrupole level, as was previously advised when anisotropic displacement parameters are assigned.[31] No local symmetry constrains were applied. In addition, anharmonicity effect on Cl atom was modeled with the refinement of the third-order coefficients of Gram−Charlier expansion using only higher order reflections as it was advised in the literature.[32] The κ and κ' parameters were employed for chlorine, carbon, and oxygen atoms. The expansion/contraction parameters of hydrogen atoms were taken from the multipolar refinement against theoretically derived structure factors (from periodic DFT/B3LYP calculations using 6-31G** basis set with the CRYSTAL06 program[33]). For both experimental and theoretical models, the same κ' parameter was used for all the valence-deformation multipoles since refinement with individual κ' for each multipole was unstable. The sequence of multipolar refinement was as follows: (1) scale factor refinement against all data, (2) high-order refinement ($\sin\theta/\lambda > 0.7$ Å^{-1}) with scale factor and third-order coefficients of Gram−Charlier expansion for Cl atom, (3) SHADE server used to obtain ADPs of hydrogen atoms further not refined, (4) refinement of population parameters together with scale factor against all data, (5) refinement of multipole parameters and scale factor with positional and thermal motions fixed, (6) refinement of expansion/contraction parameters and scale factor with all other parameters fixed, (7) refinement of all parameters with κ' parameters fixed. The difference mean-square displacement amplitudes (Δ-msda) for all bonds involving non H-atoms were within the Hirshfeld limits (mean and largest Δ-msda were 3 and 6 × 10^{-4} Å^2, respectively).[34] All static deformation and Laplacian maps as well as gradient field trajectories of total electron density were plotted using the XDGRAPH option.[27] Isosurface plots were obtained by using the MolIso program,[35] and the exact experimental electrostatic potentials were calculated by using the EP/MM method[36] as implemented in XD2006.

2.3. Theoretical Section. Ab initio calculations of the isolated molecule were performed with the Gaussian03 package at the B3LYP and 6-311++G** levels using experimental (X-ray) geometry of the chlorokojic acid molecule. The wave function (gas phase, single point) obtained this way was further used as an input file for AIMAll package,[37] which gave a full description of the topology of electron density within isolated molecule. Summary of topological analysis of electron density within isolated molecule is given in Table S2 in the Supporting Information.

dx.doi.org/10.1021/jp3058614 | J. Phys. Chem. A XXXX, XXX, XXX−XXX

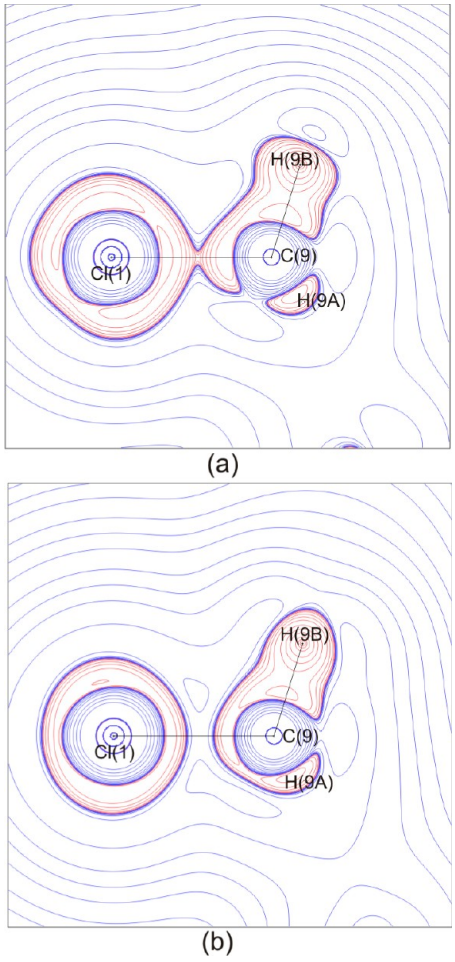

Figure 3. Experimental (a) and theoretical (periodic calculations) (b) Laplacian maps around the chlorine atom in chlorokojic acid. Contours are at logarithmic intervals in $-\nabla^2\rho(\mathbf{r})$ e·Å^{-5}.

The nature of the intermolecular interactions (together with those involving chlorine atom) has been studied by means of deformation density using periodic DFT calculations, which were performed at the B3LYP and 6-31G** levels using CRYSTAL06 program.[33] This basis set has proven to give reasonable results in the case of intermolecular interactions.[38,39] The atomic coordinates were those determined from experimental diffraction data, positions of all atoms were kept frozen. Static structure factors were computed from the resultant wave functions up to the same resolution as that observed from experiment and used in refinement with XD2006 package. No thermal or positional parameters were refined in this model. Multipolar refinement on theoretical data was carried out up to the same level as the one used for the experimental charge density modeling to compare obtained results with the experimental structure factors.

3. RESULTS AND DISCUSSION

3.1. Molecular Structure and Crystal Packing. An ORTEP view of chlorokojic acid with labeling scheme, taken from the multipolar refinement, is given in Figure 1. Table 2 contains selected geometrical parameters of the molecule obtained from low-temperature X-ray diffraction data. Those values are compared with previously reported experimental studies on crystal structure of chlorokojic acid[18] and theoretical[18,40] geometry optimization for isolated molecules of the acid. In general, the C9−Cl1 bond length obtained from theoretical calculations is elongated comparing to the one from the experiment. It seems that the experimental data are not significantly influenced by thermal motions (see footnote under Table 2). The crystal packing of the chlorokojic acid, in reference to the paper of Hryniewicz et al.,[18] shows apparent molecular ribbons built of molecules related by 2-fold screw axis and joined by O8−H8···O7 ($-x + 1, -y + 1, z + 1/2$) hydrogen bonds. The ribbons interact through weak intermolecular interactions of C−H···O and C−H···Cl type. Those weak intermolecular interactions appear to play an important role in the formation of the crystal. Their full description will be given later.

3.2. Electron Density and Topological Analysis of Chemical Bonding. The static deformation density maps obtained from experimental and theoretical multipolar refinements for the chlorokojic acid molecule in a plane of pyran ring are presented in Figure 2. Both maps show the charge build up in all covalent bonds and display all the expected subtle bonding features like lone pair regions on oxygen atoms O1, O7, and O8. It was suggested earlier[18] that there is an intramolecular hydrogen bond O8−H8···O7 (O8···O7 = 2.800(1)Å, H8···O7 = 2.42 Å, ∠O8H8O7 = 110°) in the structure of chlorokojic acid. From the Figure 2a, it can be seen that, for the carbonyl oxygen atom O7, there is no displacement

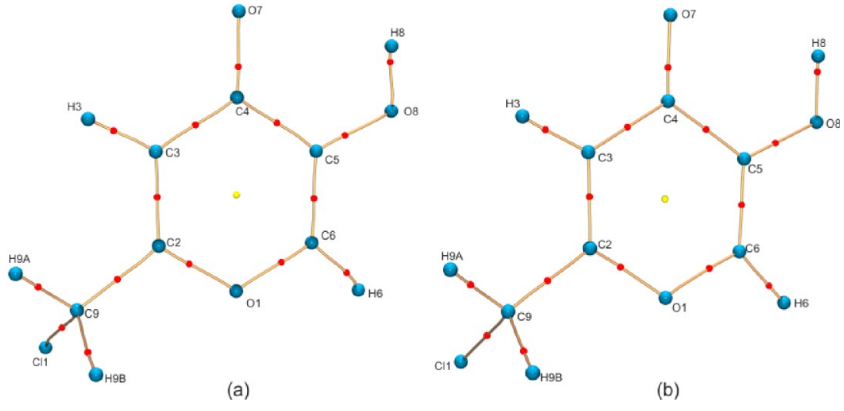

Figure 4. Molecular graphs based on experimental data (a) and periodic calculations (b), showing bond paths and bond critical points in chlorokojic acid with labeling scheme. Blue spheres indicate the atomic positions, red spheres the (3,−1) bond critical points in $\rho(r)$, and yellow sphere the (3,+1) ring critical point.

dx.doi.org/10.1021/jp3058614 | J. Phys. Chem. A XXXX, XXX, XXX−XXX

of the lone pair toward H8 atom, which suggests that there is no such intramolecular hydrogen bonding. Similar behavior appears more prominently in the theoretical static deformation maps in Figure 2b. Moreover, the topological analysis of charge density distribution using QTAIM theory for both experimental and periodic calculations indicated a lack of bond critical point between O7 and H8 atoms.

It was recently shown[43] that, if the chlorine atom lies in the same plane as the aromatic ring, the asphericity of charge density around the chlorine atom is due to a polar flattening effect. For chlorokojic acid, this is not the case since chlorine atom from chloromethyl substituent does not lie on the same plane as the pyran ring. However similar behavior was already observed in the article by Hathwar and Guru Row[43b] in 2-chloro-3-chloromethyl-8-methylquinoline where one of the chlorine atoms is not lying in the same plane as the rest of molecule. The aspherical nature of the charge density distribution around the Cl atom in chlorokojic acid is shown on experimental and theoretical Laplacian maps in Figure 3. It is worth to mention here the significant differences in the features on the Laplacian maps around the chlorine atom in both experimental and theoretical studies. This problem was already discussed in earlier studies.[43] It has been explained as a result of inadequacy of the theoretical basis sets associated with halogen atoms. Despite of the discrepancies, further studies on topology of electron density (see section 3.4) in the area of halogen interactions indicate quite good agreement in both experimental and theoretical calculations.

Topological analysis of electron density revealed that all expected BCP corresponding to covalent bonds are observed, including one (3,+1) ring critical point (RCP) at the centroid of the pyran ring characterized by $\rho(\mathbf{r})$ = 0.1736 e·Å^{-3} (*0.1320 e·Å^{-3}*) and $\nabla^2\rho_{BCP}$ = 3.1 e·Å^{-5} (*4.0 e·Å^{-5}*). The experimental and theoretical molecular graphs with the shapes of bond paths and position of bond critical points in chlorokojic acid are shown in Figure 4. The results of topological analysis from the experiment together with theoretical values are listed in Table S1 in the Supporting Information.

It is also worth noting that the values of Laplacian of electron density in chlorokojic acid can be correlated with the directions of previously observed nucleophilic attacks.[12−14] The highest value of Laplacian on the C6−H6 bond (−21.39(7) e·Å^{-5}) indicates a secondary amine attack in that position, whereas a rather low value of Laplacian on the C9−Cl1 bond (−0.69(7) e·Å^{-5}) suggests the replacement of chlorine by anions like I^- or SCN^-. Further studies on this issue are under development.

3.3. Properties of Electron Density for Hydrogen Bonding and Weak Closed-Shell Interactions. To facilitate the discussion of intermolecular contacts in chlorokojic acid, a Hirshfeld surface analysis[44] was performed with the use of CrystalExplorer.[45] These plots provide a unique signature for a molecule in crystal structure because of strong dependence on the crystalline environment of the molecule. The Hirshfeld surface for chlorokojic acid from experimental data is shown in Figure 5a. The surface is mapped as a geometrical function of d_{norm}, which combines the internal d_i and external d_e distances from the Hirshfeld surface to the nearest nucleus. Contact zones shorter than van der Waals radii are marked as red areas. Plots depict the relative contributions to the Hirshfeld surface areas due to O···H, C···H, Cl···H, H···H, Cl···Cl, and other intermolecular contacts. From this quantitative analysis together with corresponding fingerprint plots (Figure 5b) for chlorokojic acid, it can be shown that the strongest interactions are those of O−H···O type: O8−H8···O7($-x + 1, -y + 1, z + 1/2$). The chart in Figure 5c indicates that the H···O contacts constitute the highest

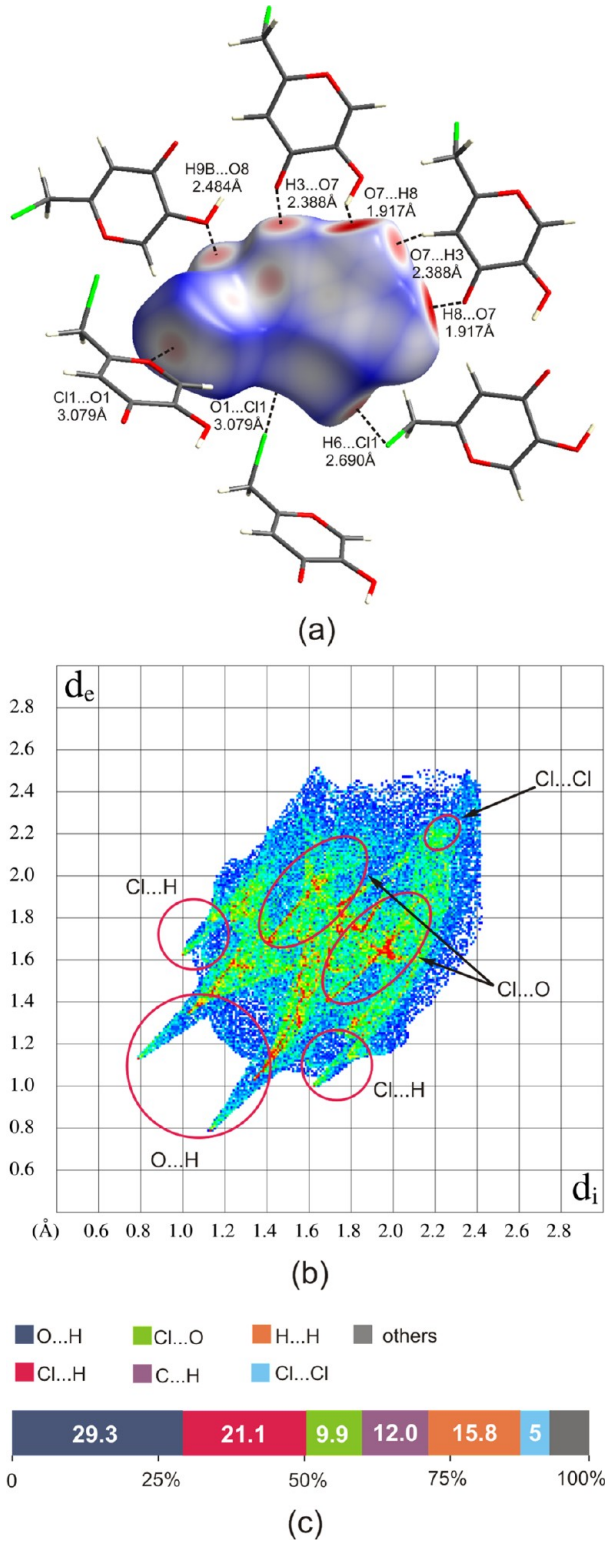

Figure 5. (a) Hirshfeld surface of chlorokojic acid mapped with d_{norm}; (b) fingerprint plot of the Hirshfeld surface. Features characteristic of key intermolecular contacts are marked in red; (c) percentage contribution to the Hirshfeld surface for the various intermolecular contacts in chlorokojic acid structure. Illustrations a and b were generated with CrystalExplorer.[45]

dx.doi.org/10.1021/jp3058614 | J. Phys. Chem. A XXXX, XXX, XXX−XXX

Table 3. Topological Analysis of Intermolecular Interactions in CP (3,−1)[a]

interaction	$\rho(\mathbf{r})$	$\nabla^2\rho(\mathbf{r})$	R_{ij}	d_1	d_2	λ_1	λ_2	λ_3	ε	$G(\mathbf{r}_c)$	$V(\mathbf{r}_c)$	$E(\mathbf{r}_c)$	$\lvert V(\mathbf{r}_c)\rvert/G(\mathbf{r}_c)$
(a)													
O8−H8···O7[b]	0.18(2)	2.69(8)	1.917	0.749	1.168	−1.37	−1.00	5.05	0.37	0.613	−0554	0.059	0.903
	0.22	*2.80*		*0.722*	*1.194*	*−1.36*	*−1.15*	*4.48*	*0.10*	*0.697*	*−0.694*	*0.003*	*0.996*
C3−H3···O7[c]	0.06(3)	1.01(1)	2.388	0.973	1.414	−0.26	−0.17	1.45	0.53	0.195	−0.137	0.058	0.703
	0.06	*0.79*		*0.968*	*1.420*	*−0.27*	*−0.20*	*1.26*	*0.34*	*0.158*	*−0.119*	*0.039*	*0.751*
C6−H6···Cl1[d]	0.04(3)	0.80(1)	2.802	1.052	1.750	−0.10	−0.10	0.99	0.06	0.147	−0.094	0.053	0.637
	0.06	*0.61*		*1.045*	*1.688*	*−0.25*	*−0.21*	*1.08*	*0.20*	*0.128*	*−0.104*	*0.024*	*0.809*
(b)													
C9−Cl1···Cl1[e]	0.03(1)	0.13(1)	4.284	2.139	2.145	−0.02	−0.02	0.17	0.13	0.023	−0.013	0.010	0.587
	0.03	*0.11*		*2.152*	*2.134*	*−0.02*	*−0.01*	*0.14*	*0.10*	*0.027*	*−0.026*	*0.001*	*0.968*
C9−Cl1···Cl1[f]	0.02(2)	0.11(1)	4.366	2.186	2.180	−0.02	−0.02	0.14	0.04	0.023	−0.018	0.005	0.781
	0.02	*0.11*		*2.179*	*2.187*	*−0.02*	*−0.02*	*0.15*	*0.02*	*0.023*	*−0.018*	*0.005*	*0.781*
C9−Cl1···Cl1[f]	0.02(3)	0.11(1)	4.366	2.182	2.182	−0.02	−0.02	0.14	0.05	0.023	−0.018	0.005	0.781
	0.02	*0.12*		*2.180*	*2.186*	*−0.02*	*−0.02*	*0.14*	*0.02*	*0.024*	*−0.018*	*0.006*	*0.762*
C9−Cl1···O1[g]	0.06(1)	0.93(1)	3.078	1.661	1.417	−0.20	−0.19	1.32	0.07	0.181	−0.130	0.051	0.718
	0.06	*0.85*		*1.634*	*1.444*	*−0.16*	*−0.16*	*1.17*	*0.03*	*0.168*	*−0.124*	*0.044*	*0.736*

[a] $\rho(\mathbf{r})$/e·Å^{-3}; $\nabla^2\rho(\mathbf{r})$/e·Å^{-5}; R_{ij}/Å; d_1,d_2, distance between BCP and atoms 1 and 2, respectively/Å; ε, ellipticity; λ_1, λ_2, λ_3/e·Å^{-5}; $G(\mathbf{r}_c)$ and $V(\mathbf{r}_c)$ are local kinetic and local potential energy density (e·Å^{-5}), respectively; $E(\mathbf{r}_c)$ is electronic local energy density (e·Å^{-5}). Abramov's expression was used to obtain local kinetic and potential energy densities.[53] (a) Hydrogen bonds, (b) Halogen interactions. Values in *italic* refer to periodic (CRYSTAL06) calculations. [b] $-x+1, -y-1, z-1/2$. [c] $-x+1, -y-1, z+1/2$. [d] $x, y, z-1$. [e] $x, y-1, z$. [f] $-x+1/2, y-1/2, z-1/2$. [g] $-x+3/2, y-1/2, z+1/2$.

Table 4. Mutual Penetration in Terms of Nonbonded Radii ($r_A°$/Å, $r_H°$/Å) and Bonded Radii (r_A/Å, r_H/Å) of Hydrogen and Acceptor Atoms

interaction	r_H	$r_H°$[d]	r_A	$r_A°$[e]	Δr_H	Δr_A	$\Delta r_H + \Delta r_A$
H8···O7[a]	0.75	1.06	1.17	1.42	0.31	0.25	0.56
H3···O7[b]	0.97	1.06	1.41	1.42	0.09	0.01	0.09
H6···Cl1[c]	1.05	1.06	1.75	1.75	0.01	0.00	0.01

[a] $-x+1, -y-1, z-1/2$. [b] $-x+1, -y-1, z+1/2$. [c] $x, y, z-1$. [d] Taken as the gas phase van der Waals radii. [e] Taken as the distance from BCP to the nucleus.

fraction (29.3%), whereas Cl···H interactions contribute in ∼21.1% and Cl···O in only ∼9.9%.

The QTAIM topological analysis indicated the amount of critical points in the area of expected O−H···O, C−H···O, and C−H···Cl interactions. In order to define above interactions as hydrogen bonds, Koch and Popelier criteria[46] were applied. The first two conditions concern the presence of a BCP between a donor and acceptor atom and the presence of charge density evaluated at the BCP, which is usually an order of magnitude smaller than the charge density at BCP found for covalent bonds. The third condition assumes that the calculated Laplacian at BCP should be positive and should correlate with interaction energies. The fourth term, which is considered as necessary and sufficient,[4,47] deals with a mutual penetration of the hydrogen atom and an acceptor. The fifth condition expresses a loss of electrons on the H-atom resulting in an increased net charge of this atom. The sixth condition, strongly related to the previous one, states the energetic destabilization of the hydrogen atom. The last two conditions suggest a decrease of dipolar polarization and volume depletion of hydrogen atoms. As was previously pointed out,[4] the first four criteria may be easily obtained from experimental data, whereas the last four require quantum-mechanical calculations for the crystal as well as for an isolated molecule. The summary of the above analysis for interactions within chlorokojic acid is given in Tables 3 and 4, theoretical values are given in parentheses in italic. For considered interactions of O−H···O, C−H···O, and C−H···Cl type, both conditions, $\Delta r_H > \Delta r_A$ and $\Delta r_H + \Delta r_A > 0$ representing the positive interpenetration of van der Waals spheres of the donor and acceptor atoms, are fulfilled.

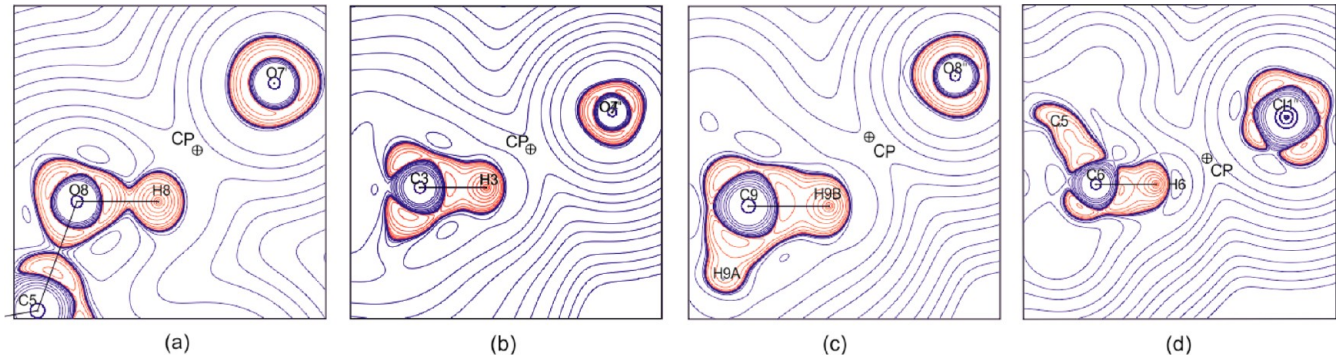

Figure 6. Experimental Laplacian maps in the area of O8−H8···O7[i] (a), C3−H3···O7[ii] (b), C9−H9B···O8[iii] (c), and C6−H6···Cl1[iv] (d) hydrogen bonds. CP, critical point. Contours are at logarithmic intervals in $-\nabla^2\rho(\mathbf{r})$ e·Å^{-5}. Symmetry codes: (i) $-x+1, -y+1, z+1/2$; (ii) $-x+1, -y+1, z-1/2$; (iii) $x, y, z-1$; (iv) $x, y, z+1$.

dx.doi.org/10.1021/jp3058614 | J. Phys. Chem. A XXXX, XXX, XXX−XXX

In Figure 6, the values of the Laplacian at the BCP are plotted against H···A distances for the studied interactions.

Another way to classify weak electrostatic interactions was proposed by Cremer and Kraka.[48] They suggested the use of electronic energy density $E(\mathbf{r}_{CP})$, defined as $G(\mathbf{r}_{CP}) + V(\mathbf{r}_{CP})$, to characterize hydrogen bonds. $V(\mathbf{r}_{CP})$ can be interpreted as the action of hydrogen bond system to the electronic charge around the critical point and $G(\mathbf{r}_{CP})$ the corresponding reaction. Following this approach, if the value of local kinetic energy density $G(\mathbf{r}_c)$ is larger than the value of local potential energy density $|V(\mathbf{r}_c)|$, the interaction is considered to be closed-shell, while if $G(\mathbf{r}_c)$ is smaller than $|V(\mathbf{r}_c)|$, the interaction is indicated to be shared. Furthermore, the larger the value of $|V(\mathbf{r}_c)|$, the more shared the interactions, and the stabilization of the structure is greater. From Table 4, it can be seen that all mentioned above interactions meet the criterion that $G(\mathbf{r}_c) > |V(\mathbf{r}_c)|$, so they can be considered to be closed-shell. Concerning the ratio of $|V(\mathbf{r}_c)|/G(\mathbf{r}_c)$, the same conclusion can be drawn using the criterion introduced by Espinosa et al.[49,50] The ratio $|V(\mathbf{r}_c)|/G(\mathbf{r}_c)$ less than 1 confirms the pure closed-shell interactions (see Table 3).

3.4. Topological Description of Halogen Interactions.

Previously,[18] it was pointed out that the chlorine atoms may form pseudohexagonal arrangement with the folded layers at 1/4, *y*, *z* and 3/4, *y*, *z* (see Figure 4b of ref 18). To confirm the existence of halogen−halogen interactions within the chlorokojic acid structure, we have carried out the topological analysis of charge density distribution in the area of those interactions. The topological analysis of both experimental and theoretical studies indicated the presence of all proposed interactions: Cl···Cl($-x + 1/2, y - 1/2, z - 1/2$), Cl($-x + 1/2, y - 1/2, z - 1/2$)···Cl($x, y - 1, z$), and Cl1···Cl1($x, y - 1, z$). The maps of gradient-vector field of total electron density from experimental and theoretical studies are presented in Figure 7. In the case of experimental data, the bond paths are curved comparing to those obtained from theoretical studies. The BCPs localized between chlorine atoms present typical properties of closed-shell interactions (Table 3b) according to Cremer and Kraka[48] and Espinosa et al.[49,50] In all cases, the magnitude of both the electron density ρ_{BCP} and the Laplacian $\nabla^2\rho_{BCP}$ are small, but as was previously shown,[51] they fall within the range of very weak hydrogen bonds. Taking into account the geometrical description of halogen−halogen interactions previously given,[51] discussed Cl···Cl interactions may refer to the X3 synthon type. The difference between the proposed model and the interactions presented in our article is that C−Cl bonds are not lying in the same plane as the Cl···Cl···Cl synthon so the angles θ_1 (180°) and θ_2 (120°) previously given are not kept. In our case θ_1 = 130.6° and θ_2 = 79.1°.

The behavior of chlorine atoms with respect to the C−Cl bond is presented on the Laplacian map plotted in the plane of one of the C−Cl···Cl−C interactions in Figure 8. The map indicates the regions of local charge concentration (CC, $\nabla^2\rho(\mathbf{r}) > 0$) and local charge depletion (CD, $\nabla^2\rho(\mathbf{r}) < 0$). CD regions are slightly shifted from the expected position along the C−Cl bond[51,52] but in front of the intermolecular $\nabla^2\rho(\mathbf{r})$ area. The look of the pseudohexagonal layer built of Cl3 synthons and its orientation in a unit cell is presented in the Supporting Information in Figure S2.

Apart from C−Cl···Cl−C weak halogen−halogen interactions, the topological analysis of charge density indicated intermolecular interaction C9−Cl1···O1 ($-x + 1, -y + 1, z - 1/2$).

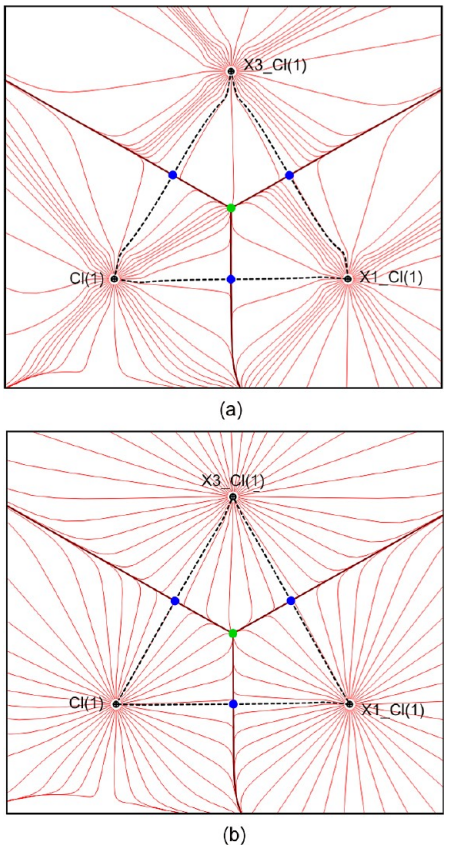

Figure 7. Gradient field trajectories of total electron density supramolecular synthons of halogen−halogen interaction obtained from experimental (a) and periodic calculations (b) data. Symmetry codes: X1_ $x, y - 1, z$; X3_ $-x + 1/2, y - 1/2, z - 1/2$.

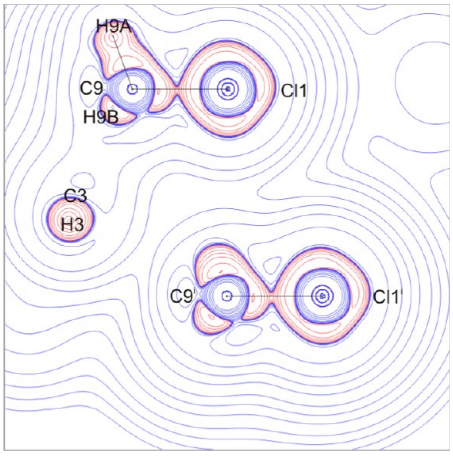

Figure 8. Halogen−halogen interaction viewed along [010] experimental Laplacian map in the area of the C−Cl···Cl−C interaction; contours are at logarithmic intervals in $-\nabla^2\rho(\mathbf{r})$ e·Å^{-5}. Symmetry codes: (i) $-x + 1/2, y - 1/2, z - 1/2$; (ii) $x, y - 1, z$.

The ρ_{BCP} and $\nabla^2\rho_{BCP}$ values at BCP are 0.06 (*0.06*) e·Å^{-3} and 0.93 (*0.85*) e·Å^{-5}, respectively, and are in a good agreement with the values recently reported by Hathwar et al.[43a] Furthermore, the interaction is considered to be closed-shell as the ratio of $|V(\mathbf{r}_c)|/G(\mathbf{r}_c)$ is found to be 0.718 (*0.736*) (see Table 4b). Moreover, the Laplacian map in the area of this interaction (Figure 9) shows similar behavior to previously discussed Cl···Cl interaction. The hole corresponding to the

dx.doi.org/10.1021/jp3058614 | J. Phys. Chem. A XXXX, XXX, XXX−XXX

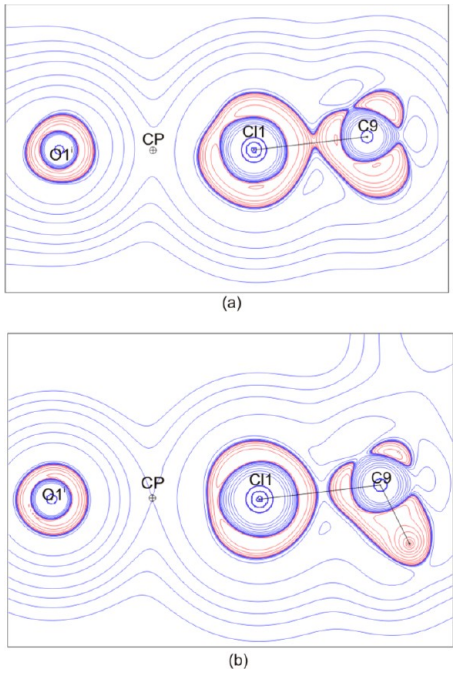

Figure 9. Experimental (a) and theoretical (periodic calculations) (b) Laplacian maps in the area of C9−Cl1···O1^{i} bond; CP, critical point. Contours are at logarithmic intervals in $-\nabla^2\rho(\mathbf{r})$ e·Å^{-5}. Symmetry codes: (i) $-x + 1/2, -y + 1/2, z - 1/2$.

charge depletion (CD) on the chlorine atom faces the local concentration (CC) on oxygen atom O1. This behavior is confirmed by periodic calculations. This feature indicates the attractive nature of C−Cl···O interactions. In addition, the total interaction energy (E_{int}) for the C−Cl···O bond was calculated as pairwise interaction energy between neighboring molecules involved in this interaction,[54] where the dispersion and exchange-repulsion terms are calculated using Williams and Cox's potential.[54] The values of E_{int} from experimental and theoretical periodic calculations are found to be −8.58 kJ/mol and −7.92 kJ/mol, respectively. All parameters describing charge density properties together with the geometrical parameters, C9−Cl1 = 1.800(1)Å, Cl1···O1 = 3.079(1)Å, and ∠C9Cl1O1=173.38(6)°, indicate the C−Cl···O interaction as being moderate and crucial for three-dimensional structure formation.

3.5. Electrostatic Potential. Electrostatic potential (ESP) has been calculated based on experimental and theoretical charge density and visualized with the MolIso program[35] (Figure 10). The most negative areas ca. −0.036 e·Å^{-1} (*−0.037 e·Å^{-1}*) are associated with the electronegative atoms, such as oxygen atoms, and suggest that they are nucleophilic, whereas the highest positive region ∼1.471 e·Å^{-1} (*1.229 e·Å^{-1}*) is concentrated at the hydrogen atom of the O8−H8 group involved in the hydrogen bond.

The most interesting feature on both maps is the quite large positive ESP region of the chlorine atom in the range of ∼0.266−0.567 e·Å^{-1}. This behavior denotes a less concentrated area of electronic charge, which is due to already mentioned (see section 3.2) anisotropy of halogen bonds. The pronounced anisotropy at Cl1, about 0.567 e·Å^{-1} along the C−Cl bond and 0.266 eÅ^{-1} perpendicular to the C−Cl direction facing away from the molecule, is in agreement with electrostatic potential isosurfaces previously observed by Politzer et al.[56] The phenomenon was explained in terms of σ-hole formation in halogen atoms along the C−X bond. Following this idea, the chlorine atom of chlorokojic acid can act both as electrophilic and nucleophilic substituents, depending on the direction: electrophiles will interact laterally with the halogen, whereas nucleophiles will interact toward the Cl−C bond direction.

4. CONCLUSIONS

The investigation of experimental charge density distribution in the structure of chlorokojic acid revealed good agreement with the theoretical periodic calculations. The topological analysis of charge density indicated the lack of a intramolecular O8−H8···O7 hydrogen bond suggested earlier. For the remaining intermolecular hydrogen bonds, O−H···O, C−H···O, and C−H···Cl types, all expected BCPs were found. It was shown that, according to the criteria by Koch and Popelier,[46,47] Cremer and Kraka,[46] and Espinosa et al.,[49,50] the hydrogen bonds have closed-shell character. Additionally, we were able to show the presence of C9−Cl1···O1 ($-x + 1, -y + 1, z - 1/2$) closed-shell intermolecular interaction with the Cl1···O1 distance of 3.079 Å.

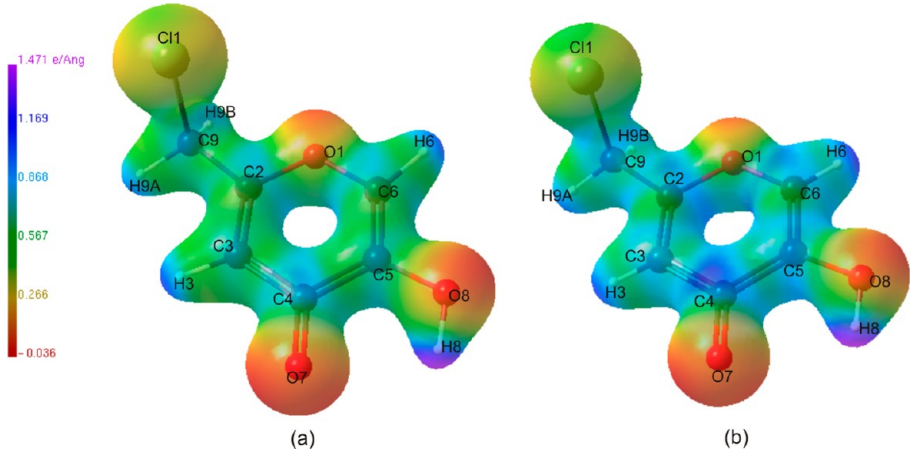

Figure 10. Electrostatic potential mapped in projections on experimental (a) and theoretical (periodic calculations) (b) electron-density isosurface at $\rho(\mathbf{r})$ = 0.5 e·Å^{-3}: apparent anisotropic distribution around the Cl1 atom. Blue and red colors represent electropositive and electronegative regions, respectively.

dx.doi.org/10.1021/jp3058614 | J. Phys. Chem. A XXXX, XXX, XXX−XXX

Concerning the halogen−halogen interactions, we have proven the presence of pseudohexagonal layers parallel to **bc** built of condensed Cl3 synthons. The topology of $-\nabla^2\rho(\mathbf{r})$ within those synthons well correlates with the short lattice parameter **b** = 4.2843(1)Å. The electrostatic potential mapped on molecular surface revealed pronounced anisotropy of Cl1 atom charge distribution. The anisotropy clarifies both electrophilic and nucleophilic properties of the chlorine atom substituent.

Recognition of electrostatic potential distribution, especially at Cl1 atom, justifies the hypothesis on the diversity of nucleophilic substitution proposed by Uher et al.[14] By diversity, we mean regular substitution of chlorokojic acid with I^- (iodokojic acid), N_3^- (azidokojic acid), and SCN^- (thiocyanato and isothiocyanato kojic acids) together with the reaction of chlorokojic acid with secondary amines. The suggestion that "abstraction of the Cl^+ ion could be facilitated by the SCN^- nucleophile, which modifies the molecular electron density distribution by interaction with the 4-one group of the pyrone skeleton and chlorine"[14] could be proved in further studies on properties of charge density distribution for chlorokojic acid derivatives obtained by such a nucleophilic substitution. Revealing the above-mentioned mechanisms might be helpful for understanding the biological activity of chlorokojic acid.

■ ASSOCIATED CONTENT

Supporting Information

CIF file; final residual maps from experimental data and periodic calculations; pseudohexagonal layer built of Cl3 synthons; topological analysis of BCPs for chlorokojic acid; topological analysis of electron density within isolated molecule of chlorokojic acid. Reference for Gaussian03. This material is available free of charge via the Internet at http://pubs.acs.org.

■ AUTHOR INFORMATION

Corresponding Author

*Tel. +48126632059. Fax: +48126340515. E-mail: krawczuk@chemia.uj.edu.pl.

Notes

The authors declare no competing financial interest.

■ ACKNOWLEDGMENTS

We thank the X-ray Laboratory, Faculty of Chemistry, Jagiellonian University, for making the Nonius KappaCCD diffractometer available. This work was partially supported by the Polish Ministry of Science and Higher Education No. N204 124 32/3169. We are grateful for valuable reviewer comments.

■ REFERENCES

(1) Bader, R. F. W. *Atoms in Molecules. A Quantum Theory*; Clarendon Press: Oxford, U.K., reprinted 1995.
(2) Koritsanszky, T. S.; Coppens, P. *Chem. Rev.* **2001**, *101*, 1583−1627.
(3) Gatti, C.; May, E.; Destro, R.; Cargnoni, F. *J. Phys. Chem. A* **2002**, *106*, 2702−2720.
(4) Munshi, P.; Guru Row, T. N. *Cryst. Rev.* **2005**, *11*, 199−241.
(5) Matta, C. F.; Boyd, R. J., Eds. *The Quantum Thoery of Atoms in Moleules: From Solid State to DNA and Drug Design*; Wiley-VCH: Weinheim, Germany, 2007.
(6) Mata, I.; Alkorta, I.; Molins, E.; Espinosa, E. *Chem.—Eur. J.* **2010**, *16*, 2442−2452.
(7) Bader, R. F. W.; MacDougall, P. J.; Lau, C. D. H. *J. Am. Chem. Soc.* **1984**, *106*, 1594−1605.
(8) Abramov, Y. A. *Acta Crystallogr.* **1997**, *A53*, 264−272.
(9) Espinosa, E.; Molins, E.; Lecomte, C. *Chem. Phys. Lett.* **1998**, *285*, 170−173.
(10) Feng, M.-H.; Van der Does, L.; Bantjes, A. *J. Med. Chem.* **1993**, *36*, 2822−2827.
(11) Dilsiz-Aytemir, M.; Demir Erol, D.; Hider, R. C.; Ozalp, M. *Turk. J. Chem.* **2003**, 757−764.
(12) Konopikowa, M.; Bransova, J.; Uher, M.; Liptaj, T.; Rajnikova, O. *Chem. Pap.* **1995**, *49*, 137−141.
(13) Uher, M.; Konecny, V.; Rajnikova, O. *Chem. Pap.* **1994**, *48*, 282−284.
(14) Uher, M.; Szymońska, J.; Korenova, A.; Tomasik, P. *Monatsh. Chem.* **2000**, *131*, 301−307.
(15) Wolf, P. A.; Westveer, W. M. *Arch. Biochem.* **1950**, *28*, 201−206.
(16) Ahmeton, M. T.; Frampton, C. S.; Silver, J. *J. Chem. Soc., Dalton Trans.* **1988**, 1159−1163.
(17) Thompson, K. H.; Orvig, C. *Coord. Chem. Rev.* **2001**, 1033−1053.
(18) Hryniewicz, K.; Stadnicka, K.; Pattek-Janczyk, A. *J. Mol. Struct.* **2009**, *919*, 255−270.
(19) Liu, Z. D.; Piyamongkol, S.; Liu, D. Y.; Khodr, H. H.; Lu, S. L.; Hider, R. C. *Bioorg. Med. Chem.* **2001**, *9*, 563−573.
(20) Nonius. *COLLECT*; Nonius BV: Delf, The Netherlands, 1997.
(21) Otwinowski, Z.; Minor, W. In *Macromolecular Crystallography*; Carter, C. W., Jr., Sweet, R. M.; Methods in Enzymology, Part A; Elsevier: New York, 1997; Vol. *276*, p 307.
(22) Blessing, R. H. *J. Appl. Crystallogr.* **1997**, *30*, 421−426.
(23) Sheldrick, G. M. *Acta Crystallogr.* **2008**, *A64*, 112−122.
(24) Farrugia, L. J. *J. Appl. Crystallogr.* **1997**, *30*, 565.
(25) Farrugia, L. J. *J. Appl. Crystallogr.* **1999**, *32*, 837−838.
(26) Hansen, N. K.; Coppens, P. *Acta Crystallogr.* **1978**, *A34*, 909−921.
(27) Volkov, A.; Macchi, P.; Farrugia, L. J.; Gatti, C.; Mallinson, P.; Richter, T.; Koritsanszky, T. *XD2006*, A Computer Program Package for Multipole Refinement, Topological Analysis of Charge Densities, and Evaluation of Intermolecular Energies from Experimental and Theoretical Structure Factors; University of Buffalo: Buffalo, NY, 2006.
(28) Allen, F. H.; Bruno, I. J. *Acta Crystallogr.* **2010**, *B66*, 380−386.
(29) Madsen, A. Ø. *J. Appl. Crystallogr.* **2006**, *39*, 757−758.
(30) Munshi, P.; Madsen, A. Ø.; Spackman, M. A.; Larsen, S.; Destro, R. *Acta Crystallogr.* **2008**, *A64*, 465−475.
(31) Hoser, A. A.; Dominiak, P. M.; Wozniak, K. *Acta Crystallogr.* **2009**, *A65*, 300−311.
(32) (a) Sorensen, H. O.; Stewart, R. E.; McIntyre, G. J.; Larsen, S. *Acta Crystallogr.* **2003**, *A59*, 540−550. (b) Hathwar, V. R.; Gonnade, R. G.; Munshi, P.; Bhadbhade, M. M.; Guru Row, T. N. *Cryst. Growth Des.* **2011**, *11*, 1855−1862.
(33) Dovesi, R.; Saunders, V. R.; Roetti, C.; Orlando, R.; Zicovich-Wilson, C. M.; Pascale, F.; Civalleri, B.; Doll, K.; Harrison, N. M.; Bush, I. J.; D'Arco, P.; Llunell, M. *CRYSTAL06, User's Manual*; University of Torino: Torino, Italy, 2006.
(34) Blessing, R. H. *J. Appl. Crystallogr.* **1997**, *30*, 421−426.
(35) Hübschle, C. B.; Luger, P. *J. Appl. Crystallogr.* **2006**, *39*, 901−904.
(36) Volkov, A.; Koritsanszky, T.; Coppens, P. *Chem. Phys. Lett.* **2004**, *391*, 170−175.
(37) Keith, T. A. *AIMAll*, version 11.09.18, 2011.
(38) Munshi, P.; Guru Row, T. N. *Acta Crystallogr.* **2006**, *B62*, 612−626.
(39) Munshi, P.; Thakur, T. S.; Guru Row, T. N.; Desiraju, G. R. *Acta Crystallogr.* **2006**, *B62*, 118−127.
(40) Zborowski, K.; Korenova, A.; Uher, M.; Proniewicz, L. M. *J. Mol. Struct.* **2004**, *683*, 15−22.
(41) Nardelli, M. *J. Appl. Crystallogr.* **1995**, *28*, 659.
(42) Busing, W. R.; Levy, H. A. *Acta Crystallogr.* **1964**, *17*, 142−146.
(43) (a) Hathwar, V. R.; Gonnade, R. G.; Munshi, P.; Bhadbhade, M. M.; Guru Row, T. N. *Cryst. Growth Des.* **2011**, *11*, 1855−1862. (b) Hathwar, V. R.; Guru Row, T. N. *J. Phys. Chem. A* **2010**, *114*,

13434−13441. (c) Hathwar, V. R.; Guru Row, T. N. *Cryst. Growth Des.* **2011**, *11*, 1338−1346.
(44) (a) Spackman, M. A.; Jayatilaka, D. *CrystEngComm* **2009**, *11*, 19−32. (b) Spackman, M. A.; McKinnon, J. J. *CrystEngComm* **2002**, *4*, 378−392. (c) McKinnon, J. J.; Spackman, M. A.; Mitchell, A. S. *Acta Crystallogr.* **2004**, *B60*, 627−668. (d) McKinnon, J. J.; Jayatilaka, D.; Spackman, M. A. *Chem. Commun.* **2007**, 3814−3816.
(45) Wolff, S. K.; Grimwood, D. J.; McKinnon, J. J.; Jayatilaka, D.; Spackman, M. A. *CrystalExplorer 2.0*; University of Western Australia: Perth, Australia, 2007; see http://hirshfeldsurface.net/CrystalExplorer.
(46) Koch, U.; Popelier, P. L. A. *J. Phys. Chem.* **1995**, *99*, 9747−9754.
(47) Popelier, P. Quantum Chemical Topology: On Bonds and Potential. In *Intermolecular Forces and Clusters*; Springer: Berlin, Germany, 2005; p 115.
(48) Cremer, D; Kraka, E. *Angew. Chem.* **1984**, *23*, 627−628.
(49) Espinosa, E.; Molins, E.; Lecomte, C. *Chem. Phys. Lett.* **1998**, *285*, 170−173.
(50) Espinosa, E.; Alkorta, I.; Elguero, J.; Molins, E. *J. Chem. Phys.* **2002**, *117* (12), 5529−5542.
(51) Thu Bui, T. T.; Dahaoui, S.; Lecomte, C.; Desiraju, G. R.; Espinosa, E. *Angew. Chem.* **2009**, *121*, 2896−3899.
(52) Tsirelson, V. G.; Zhou, P. F.; Thang, T.-H.; Bader, R. F. W. *Acta Crystallogr.* **1995**, *A51*, 143−153.
(53) Abramov, Y.; Volkov, A.; Wu, G.; Coppens, P. *Acta Crystallogr.* **2000**, *A56*, 585−591.
(54) Williams, D. E.; Cox, S. R. *Acta Crystallogr.* **1984**, *B40*, 404−417.
(55) Flack, H. D. *Acta Crystallogr.* **1983**, *A39*, 876−881.
(56) Politzer, P.; Lane, P.; Concha, M. C.; Ma, Y.; Murray, J. S. *J. Mol. Model.* **2007**, *13*, 305−311.